Kinetics of Nonideal Hyperbranched Polymerizations. 2. Kinetic Analysis of the Polycondensation of 3,5-Bis(trimethylsiloxy)benzoyl chloride Using NMR Spectroscopy†

Dirk Schmaljohann,‡ Hartmut Komber,‡ Joshua G. Barratt,§ Dietmar Appelhans,‡ and Brigitte I. Voit*,‡

Institute of Polymer Research, Hohe Strasse 6, 01069 Dresden, Germany, and Cornell University, Department of Theoretical and Applied Mechanics, Ithaca, New York 14853

Received June 21, 2002

ABSTRACT: The kinetics of the polycondensation of 3,5-bis(trimethylsiloxy)benzoyl chloride (**BTMSBCl**) was investigated. 1D and 2D NMR techniques were applied to achieve a complete signal assignment of the structural units of the resulting polymer (poly(3,5-dihydroxybenzoic acid), **PDHBA**), which was obtained after hydrolysis of the trimethylsiloxy and the acid chloride groups. Furthermore, the diads could be identified. After quantification of the signals by ^{13}C NMR spectroscopy, a data set of ratios of structural units as a function of the conversion had been studied with respect of the kinetics of the system and their resulting structural composition. Since the data do not follow the ideal conversion dependence, the relative rate constants of the 12 different basic reaction steps were determined by simulation, which fit the obtained data best. A study of the sensitivity of the reaction curves to changes in the individual rate constants showed large differences and helped to distinguish the importance of the different basic reactions to the overall reaction. One kinetic situation was identified as dominant. The deviations (from the ideal conversion dependence) were explained by different electronic effects on the reaction sites caused by the successive substitution of siloxy and benzoyl chloride groups by ester groups on the aromatic ring. Analysis of the data for the diads indicated no further kinetic effect.

Introduction

Hyperbranched polymers build a class of polymer architectures derived from a multifunctional monomer AB_n. A three-dimensional branched polymer molecule is formed with some unique properties such as a globular structure and a large number of functional groups. As Flory pointed out in 1952, a cross-linking for an AB_2 system would take place exactly at 100% conversion of the **A** function. Flory was the first to discuss the theory of hyperbranched polycondensation.[1] His studies on the branching coefficent α and the molecular weight distribution focused on systems, where the reactivity and the probability for a reaction at a particular position does not change along the reaction pathways. Fréchet et al.[2] and Kim et al.[3] introduced the definition of the degree of branching (DB) by comparing the hyperbranched polymers with their perfectly branched analogues, the dendrimers. More recent works by Müller et al.,[4−7] Frey et al.,[8−10] Möller et al.,[11] Dušek et al.,[12] Fawcett et al.[13,14] and Galina et al.[15] started a detailed discussion of the theory. Müller studied the molecular weight distribution and the conversion dependence of the structural units and molecular parameters, whereas Frey defined a new degree of branching DB (compare with eq 7). These equations were derived with the assumption that all reaction steps proceed with the same rate constant *k*. The final product contains 50% **L** units and 25% **T** and **D** units, respectively. (**T** = terminal unit, **L** = linear unit, **D** = dendritic unit; the notation of the units in capital letters only distinguishes between different substituents on the B_2 site but not on the **A** site for an AB_2 monomer.) Within this paper we will refer to this particular kinetic situation as the ideal situation.

Recently we were able to confirm the theoretical equations of Müller et al.[5] and Frey et al.[9] with NMR data from the polycondensation of 4,4-bis(4′-hydroxyphenyl)pentanoic acid.[16] The reaction sites of this monomer are well separated such that neither electronic nor steric effects influence the reactivity. Thus, every reaction of a structural unit is only based on the probability of its occurrence and even the diads do not show any deviation from the ideal distribution indicating second-order effects through steric requirements.

Since not every real system exhibits well-separated reaction sites, there is more interest in the description of polycondensations and polymerizations with nonuniform reaction rate constants. A first approach to discuss AB_2 systems with unequal reaction rates has been made by Frey et al.[9] In their study, they distinguished two different reaction steps, from terminal to linear unit (k_T) and from linear to dendritic unit (k_L), respectively. The ratio of the two different reaction rate constants was defined as factors $x = k_L/k_T$, which influences the DB of the final product. Müller et al.[5,7] presented a similar description for the self-condensing vinyl polymerization, which can be considered as a special situation of an ABB′ system. Again a ratio of different rate constants was introduced and discussed. We chose a different approach for the description of the hyperbranched polymerization: all basic reaction steps were identified, and each step has its own reaction rate constant. This allows the discussion of different kinetic situations and one can easily extend the analysis to other kinetic systems. A detailed discussion of this approach was given in a preceding paper.[17]

† Part 1: Schmaljohann, D.; Barratt, J. G.; Komber, H.; Voit, B. I. *Macromolecules* **2000**, *33*, 6284.
‡ Institute of Polymer Research.
§ Cornell University.

10.1021/ma020972m CCC: $25.00
Published on Web 12/02/2002

Scheme 1

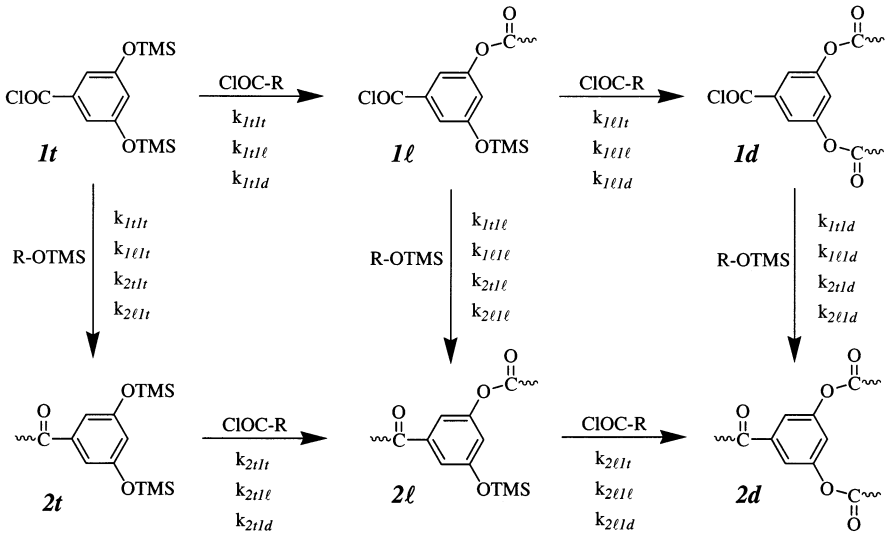

Table 1. Changes of the Structural Units along One Row or Column of the K Matrix, Respectively[a]

$1t + 1t \xrightarrow{k_{1t1t}} 1\ell + 2t$	$1\ell + 1t \xrightarrow{k_{1\ell1t}} 1d + 2t$	$2t + 1t \xrightarrow{k_{2t1t}} 2\ell + 2t$	$2\ell + 1t \xrightarrow{k_{2\ell1t}} 2d + 2t$	$\Rightarrow \quad 1t \rightarrow 2t$
$1t + 1\ell \xrightarrow{k_{1t1\ell}} 1\ell + 2\ell$	$1\ell + 1\ell \xrightarrow{k_{1\ell1\ell}} 1d + 2\ell$	$2t + 1\ell \xrightarrow{k_{2t1\ell}} 2\ell + 2\ell$	$2\ell + 1\ell \xrightarrow{k_{2\ell1\ell}} 2d + 2\ell$	$\Rightarrow \quad 1\ell \rightarrow 2\ell$
$1t + 1d \xrightarrow{k_{1t1d}} 1\ell + 2d$	$1\ell + 1d \xrightarrow{k_{1\ell1d}} 1d + 2d$	$2t + 1d \xrightarrow{k_{2t1d}} 2\ell + 2d$	$2\ell + 1d \xrightarrow{k_{2\ell1d}} 2d + 2d$	$\Rightarrow \quad 1d \rightarrow 2d$
$\Downarrow$	$\Downarrow$	$\Downarrow$	$\Downarrow$	
$1t \rightarrow 1\ell$	$1\ell \rightarrow 1d$	$2t \rightarrow 2\ell$	$2\ell \rightarrow 2d$	

[a] The first number−letter combination gives the structural unit reacting on the **B** site, the second combination denotes the unit reacting on the **A** site; all reactions along one row or column, respectively, give the reaction of a particular pathway.

This theoretical work was stimulated by the fact that the polycondensation of a monomer like 3,5-bis(trimethylsiloxy)benzoyl chloride results in a hyperbranched polymer with a DB larger than 50%, the final value of the ideal situation. In 1991, Fréchet et al.[2] published the polycondensation of 3,5-bis(trimethylsiloxy)benzoyl chloride (**BTMSBCl**) and they reported a DB of 60% for the resulting poly(3,5-dihydroxybenzoic acid) (**PDHBA**). **PDHBA** was isolated after hydrolysis of the moisture-sensitive trimethylsiloxy and acid chloride groups. During our studies on the modification of **PDHBA**, we found a DB in the same range of 60−64%.[18] An activation or deactivation of the different reaction sites is possible due to different electron densities caused by different substituents formed in the course of the reaction. Differences in the inductive effects of the substituents is a possible reason for such changes in the electron density. Since all reaction sites are located at one benzene ring, steric hindrance has to be considered as well. Other examples for nonideal polycondensation reaction are also known: Thompson et al.[19] discussed the polycondensation of a protected 3,5-dihydroxyphenyl-4-fluorophthalimide leading to a hyperbranched poly(etherimide) with a DB of 66−67%. (Different DB values occur when using different equations: Fréchet, DB = $(T + D)/(T + L + D)$; Frey, DB = $2D/(L + 2D)$.) In their cases, the conversion from a silyl ether to an aryl ether leads to an increase in reactivity, which then raises the ratio of branching units above the statistical expected value. One example of a lower DB is given by Hult et al.;[20] they investigated the polycondensation of 2,2-bis(hydroxymethyl)propionic acid (bis-MPA) and reported DB = 32−35% due to hindered accessibility of the reacting groups. All these results give rise to the question of how to describe a system which does not behave like the ideal system.

In the following, we will shortly introduce the reaction paths of **BTMSBCl** and the resulting structural units of **PDHBA** as our studied AB_2 system and the notation we used.

Taking the influence of all three reaction sites into account, one can see that the six different structural units are connected with each other via seven reaction paths (Scheme 1). These seven pathways represent the 12 basic reactions, which are shown in Table 1. We will use a number−letter combination for the notation of the six structural units.

The number "**1**" indicates that the **A** function (acid chloride) has not reacted, whereas "**2**" stands for the formed phenyl ester at the **A** site. The letters "**t**", "**l**" and "**d**" denote the terminal, linear, and dendritic unit, respectively, depending upon whether zero, one or two **B** functions (trimethylsiloxy group) have reacted. The main structural units are indicated with capital letters (**T**, **L** or **D**) and they cover both "**1y**" and "**2y**" structure units, e.g. **T** = **1t** + **2t**.

The polycondensation of an AB_2 system with nonuniform reaction rate constant is described by a 3 × 4 **K** matrix of k values. The columns give a set of reactions, where a particular **B** site is reacting with the **A** function of the structural units, and the rows give a set of reactions reacting at a particular **A** site (compare Table 1 and Scheme 1):

$$\mathbf{K} = \begin{bmatrix} k_{\mathbf{1t1t}} & k_{\mathbf{1l1t}} & k_{\mathbf{2t1t}} & k_{\mathbf{2l1t}} \\ k_{\mathbf{1t1l}} & k_{\mathbf{1l1l}} & k_{\mathbf{2t1l}} & k_{\mathbf{2l1l}} \\ k_{\mathbf{1t1d}} & k_{\mathbf{1l1d}} & k_{\mathbf{2t1d}} & k_{\mathbf{2l1d}} \end{bmatrix} \tag{1}$$

This paper describes the kinetic analysis of the polycondensation of 3,5-bis(trimethylsiloxy)benzoyl chloride (**BTMSBCl**). The contents of different structural units at different degrees of conversion were obtained from quantitative ^{13}C NMR spectra. The signal assignment for the resulting polymer **PDHBA** given in this paper is based on a detailed spectra analysis through a combination of different NMR techniques. It is noteworthy that we describe the kinetics of the polycondensation of the monomer **BTMSBCl**, but the analysis has been carried out on the product of the subsequent complete hydrolysis of all TMS and acid chloride groups to hydroxy and carboxylic acid groups, respectively, because these groups are moisture sensitive and its quantification might introduce errors due to partial hydrolysis. The kinetics of this system has been studied and we were able to fit our data by numerical evaluation to a set of different reaction rate constants. Besides the discussion of our experimental data, we like to conceptualize the chosen approach, which eventually can be applied to other kinetic systems.

Experimental Section

Sample Preparation. The monomer synthesis was carried out according to the method of Kricheldorf et al.[21] The polycondensation reaction has been done similar to the method of Fréchet et al.[2] The monomer was mixed in a Schlenk flask with 1 wt % NEt_4Cl. The reaction was carried out at 170 °C in a slow N_2 stream. Samples were continuously taken out of the flask over 36 h. The polymer was dissolved in THF, then water was added to the solution to hydrolyze the remaining silyl ether and acid chloride functions to the corresponding phenols and carboxylic acids, respectively. After a 3 h stirring of the THF solution, the polymer **PDHBA** was isolated by evaporating the solvent and drying the samples in a vacuum over P_2O_5.

NMR Experiments. The NMR spectra were obtained on a Bruker DRX 500 spectrometer operating at 500.13 MHz for ^1H and 125.77 MHz for ^{13}C. Here, 0.5 M solutions (referring to the molecular weight of a linear unit) in DMSO-d_6 (lock and internal standard, $\delta(^1H) = 2.50$ ppm, $\delta(^{13}C) = 39.6$ ppm) were measured at 303 K. The ^{13}C spectra were obtained using inverse gated decoupling, $\pi/2$ ^{13}C pulses and a pulse delay of 12 s (at least 5 times the longest T_1). The T_{1C} values were determined by the inversion recovery method using 10 τ values and a pulse delay of 12 s. The relative errors for T_{1C} values were estimated to 10%. The error in determining the mole fractions of the different units from a NMR spectrum is ≤2 mol % depending on the signal-to-noise ratio for the individual signal. This value was determined from repeated measurements, integrations and deconvolutions. $^1H-^1H$ and $^1H-^{13}C$ shift-correlated spectra were recorded using the standard pulse sequences provided by Bruker.

Simulation and Fit of the Data. Simulation of the curves has been carried out using an iterative process. Each step is normalized to the conversion of **A** groups (p_A) and counts $0.001p_A$ giving 1000 steps of iteration. The fit of the experimental data has been done using a Newton search method with quadratic estimates and central derivatives. Only those values, which still exceed the experimental error of $0.02 \cdot A_0$ (every concentration of structural units is normalized to the initial concentration of **A** groups A_0), were minimized for the final determination of the **K** matrix. The sensitivity matrix **E** was calculated applying an "error" for the k values of $k_{\beta\alpha}' = k_{\beta\alpha}(1 + 10^{-8})$ followed by a numerical integration of the generated conversion curves over 1000 steps. At each step, the value was squared and after summation over all steps and over each of the six structural units the sensitivity values were normalized to $\epsilon(k_{\mathbf{1t1t}})$ (vertical least-squares minimization over the data points).

Scheme 2

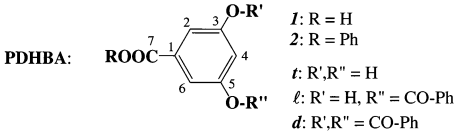

1: R = H
2: R = Ph

t: R',R" = H
l: R' = H, R" = CO-Ph
d: R',R" = CO-Ph

Results and Discussion

The first use of 3,5-bis(trimethylsiloxy)benzoyl chloride (**BTMSBCl**) as a branching unit in polycondensations was done by Kricheldorf et al.,[21] the first homopolycondensation of **BTMSBCl** has been published by Fréchet et al.[2,22] We performed the reaction similar to the previously described polycondensation, but in a way avoiding distillation of the monomer out of the flask, as well as fractionation of the sample during workup. Workup included a complete hydrolysis of the TMS and acid chloride groups resulting in the polymer poly(3,5-dihydroxybenzoic acid) (**PDHBA**). A characterization and analysis of the polymer properties has been given elsewhere.[2,22,23] We extended the NMR analysis, which was necessary for an accurate determination of the ratios of structural units as a function of conversion.

NMR Spectroscopy. In a preceding paper, we have demonstrated the use of ^{13}C NMR spectroscopy in quantifying the structural units of hyperbranched polyesters with different degrees of polymerization ($\bar{P}_n$).[16] With the same goal, we were interested in an extensive ^{13}C NMR signal assignment for poly(3,5-dihydroxy benzoic acid) (**PDHBA**) with respect to signals characteristic for the different structural units **1t**, **1l**, **1d**, **2t**, **2l**, and **2d**.

A first ^1H and ^{13}C NMR signal assignment for **PDHBA** was reported by Fréchet et al. based on spectra of model compounds.[2] The signals, which are characteristic for **2t**, **2l**, and **2d** units, could be identified. Furthermore, it was mentioned that the peaks reveal a degree of fine structure, but a detailed signal assignment was not undertaken.

The aim of our NMR investigation is to assign these fine structure signals for **PDHBA** with a high $\bar{P}_n$. In addition, we are also interested in finding structure-characteristic signals for products with low $\bar{P}_n$ where besides the units **2t**, **2l**, and **2d** the units **1t**, **1l**, and **1d** are also of significant amount. For this reason a combined analysis of ^1H, ^{13}C, $^1H-^1H$ shift-correlated (COSY), and $^1H-^{13}C$ one- and multiple-bond shift correlated (HMQC, HMBC) spectra of samples with different $\bar{P}_n$s was carried out. We do not describe this analysis in detail but discuss the result with respect to quantitative structural analysis. The atom numbering corresponds to Scheme 2.

Figure 1 shows the 500 MHz ^1H NMR spectrum of **PDHBA** at high conversion of **A** groups p_A ($p_A \approx 1$) in DMSO-d_6, which is quite complex. The signal groups in the spectrum shown can be assigned to different protons of the main structures **2t**, **2l**, and **2d**.

The signal fine structures are caused by the type of the preceding *and*, for **2l** and **2d**, of the following structural unit. The para-effect due to different preceding units (**2l** or **2d**) yields two signals of H_4(**2t**) with a chemical shift difference of 0.01 ppm. So, the larger chemical shift differences between the three signals of H_4(**2l**) (0.05 ppm) and the five signals of H_4(**2d**) are due to different R′ and the possible combinations of different R′ and R″, respectively. For $H_{2/6}$ the ortho- and para-effects due to different R′ and R″-substitution yield a

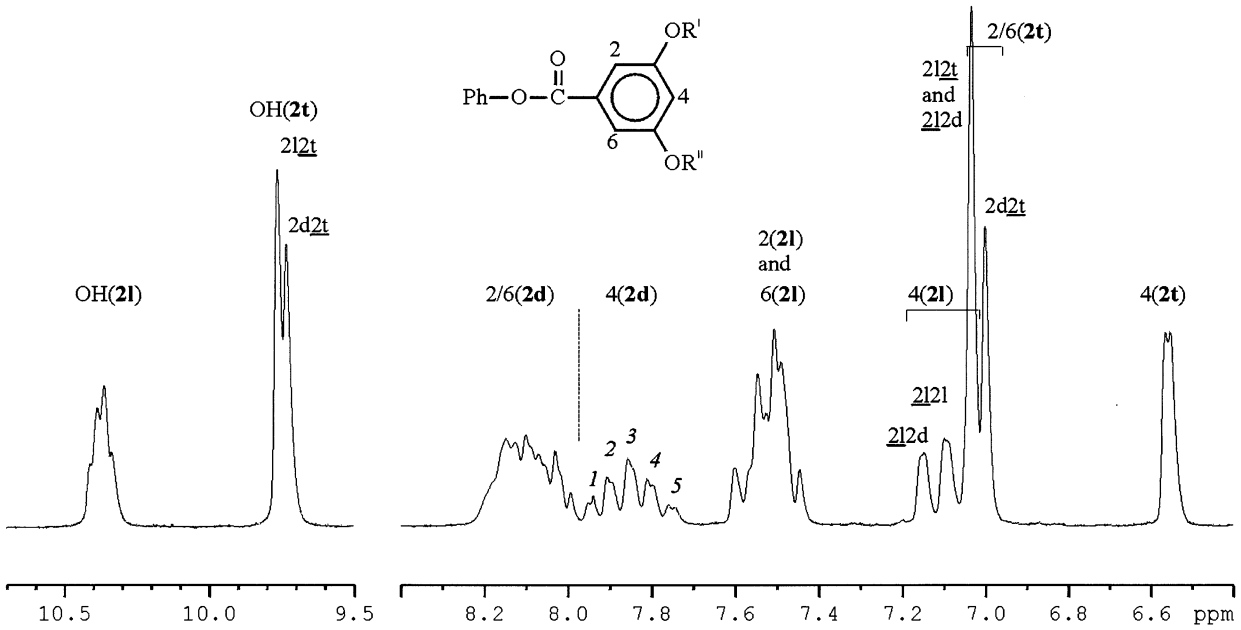

Figure 1. 500 MHz ^{1}H NMR spectrum of **PDHBA** ($p_A \approx 1$) in DMSO-d_6. with assignments to the different structural units and partly to the diads (proton in the underlined structural unit) Signal assignment for 1−5 of 4(**2d**): (1) R′ = R″ = **2d**; (2) R′ = **2d**, R″ = **2l**; (3) R′ = R″ = **2l** and R′ = **2d**, R″ = **2t**; (4) R′ = **2l**, R″ = **2t**; (5) R′ = R″ = **2t**.

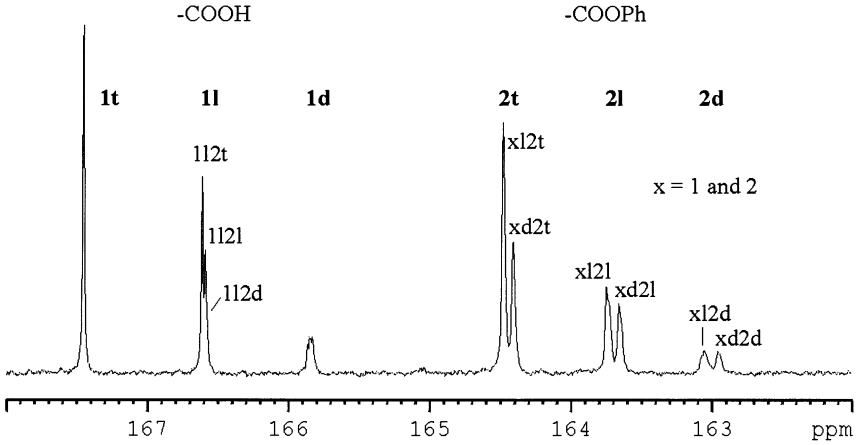

Figure 2. 125 MHz ^{13}C NMR spectrum (region of the carbonyl carbons) of **PDHBA** ($p_A = 0.573$) in DMSO-d_6.

more complicated spectrum for **2l** and **2d**. Further chemical shift effects occur for oligomers with **1t**, **1l**, and **1d** units. A detailed signal assignment was therefore not undertaken. For some oligomers dissolved in carefully dried DMSO-d_6, **1l** and **1t** units can also be identified besides **2l** and **2t** by their phenolic protons which result in signals at 10.15 ppm for **1l** and 9.50 ppm for **1t**. Therefore, the ^{1}H NMR spectrum gives a first possibility to quantify structural units also for a conversion of **A** groups $p_A < 1$. However, **1d** and **2d** units, which show the most complex fine structure, cannot be quantified due to signal overlap.

For a complete structure characterization ^{13}C NMR was used. Fortunately, the carbonyl signal region (Figure 2) gives all information to describe the hyperbranched structure of oligomers and polymers on the level of the six structural units **1(t, l, d)** and **2(t, l, d)** and also the content of diads **z2(t, l, d)** (**z** = **L** or **D**) can be determined. The structure of these diads is shown in Scheme 4. The fine structure of the COOH carbon of **1l** and **1d** indicates that even chemical shift effects due to different structural units in R′ and R″ position can be observed. However, these effects are less

Scheme 3

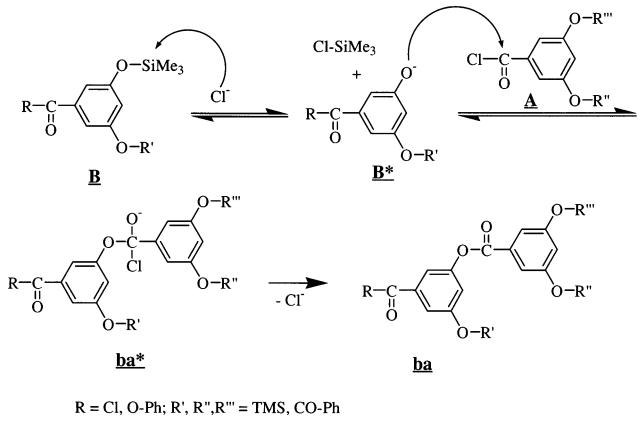

than 0.03 ppm and could only be assigned for **1l** (three signals due to the diads **1l2t**, **1l2l**, **1l2d**). The diad signal assignment has been achieved by comparison of the intensity ratio within a pair of diad signals with the **D**/**L** intensity ratio of the structural units. This was done on several samples with different ratios of structural

Scheme 4

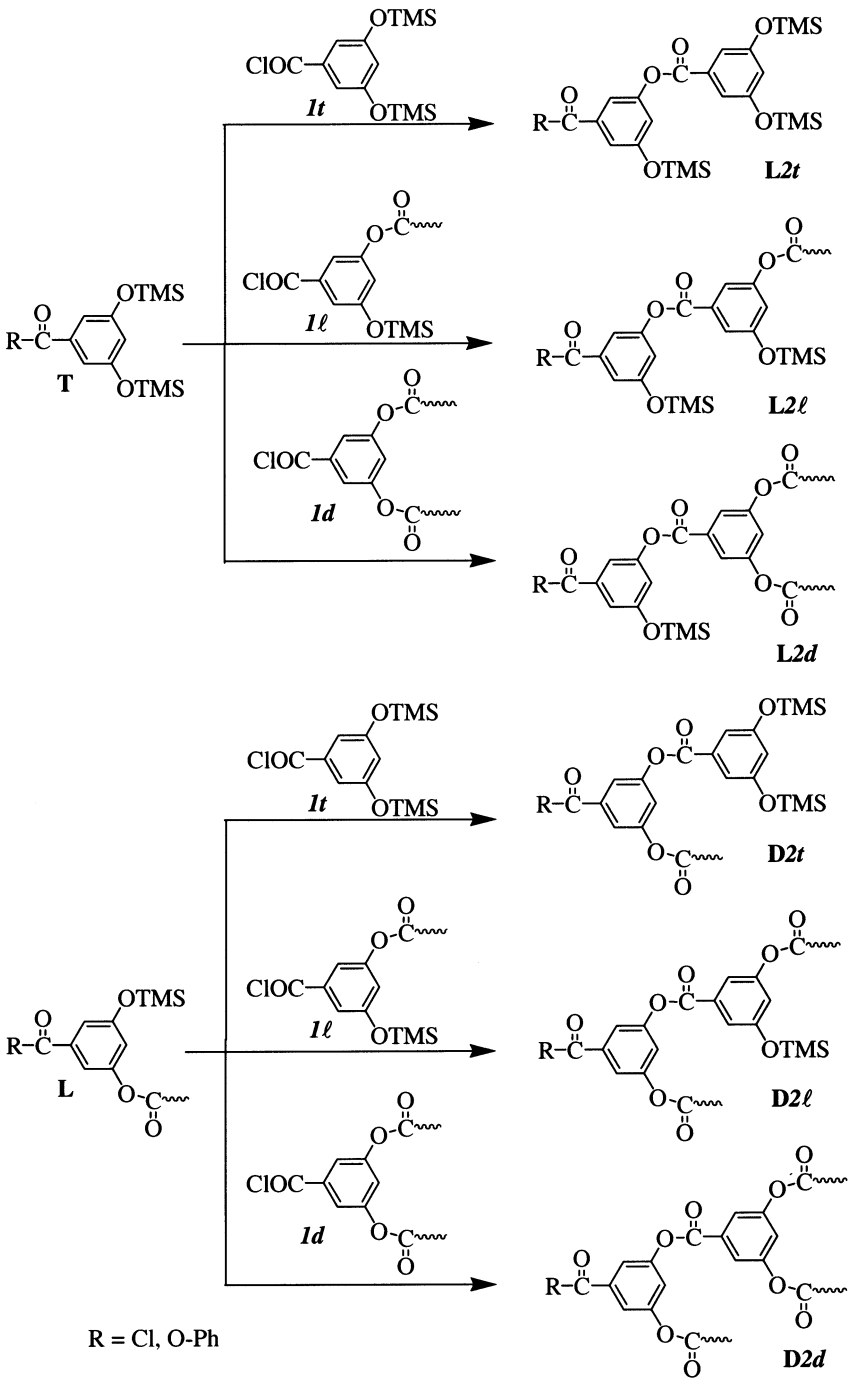

units. For oligomers the signal groups of the aromatic carbons are characterized by an overlapping of the signals due to **1** and **2** units in different diads and triads, which complicates the quantification. This is not surprising taking into account the minor structure differences and so chemical shift effects due to the different structural units. Values smaller than 0.4 ppm are characteristic for sequence effects in aromatic polyesters.[16,24] Some characteristic signals for **1** units are given in Table 2. Thus, the carbon directly bonded to the COOH group shows three separated signals due to **1t**, **1l**, and **1d**.

For products with a high degree of conversion, where the content of **1** units can be neglected, more signal groups can be analyzed with regard to the content of **2(t, l, d)** units and their diads. For such a polymer the aromatic carbons region of the ^{13}C NMR spectrum (Figure 3) and all ^{13}C signal assignments (Table 2) are given. Also shift increments both for **2l** relative to **2d** on the following unit and for **2t** and **2l** relative to **2d** on the preceding unit were reported (0.1−0.26 ppm) in Table 2. Fortunately, the meta-effects are the same for all units, which is the reason for the less complex fine structure for C_1 and $C_{3/5}$ of **2d** and C_1 and C_5 of **2l**. In contrast, the other ring carbons of both units show a complex fine structure due to different triads. For **2t** only the preceding unit (**2l** or **2d**) causes a chemical shift effect and results in two different signals for C_1, $C_{2/6}$, and C_4. A characteristic feature of the spectra is increasing line width going from **2t** to **2d** units and also from **2l2t** to **2d2d** diads. This effect was also described in our ^{13}C relaxation time study on a hyperbranched

Table 2. Assignment of the ^{13}C NMR Signals of the 2 Units, Their T_{1C} Values and Characteristic Signals of 1 Units

carbon atom[a]	**2t** (δ, ppm)	**2l** (δ, ppm)	**2d** (δ, ppm)	T_{1C}[b] (s)	further assignments (δ, ppm)
COOR	164.43 (**2l2*t***)	163.68 (**2l2*l***)	163.00 (**2l2*d***)	1.3	167.45 (**1t**); 166.61 (**1l**)
(**2**: R = Ph; **1**: R = H)	164.36 (**2d2*t***)	163.61 (**2d2*l***)	162.92 (**2d2*d***)		165.83 (**1d**)
1	130.28 (**2l2*t***)	130.75 (**2l2*l***)	131.18 (**2l2*d***)	1.1	132.62 (**1t**); 132.99 and 132.96 (**1l**);
	130.00 (**2d2*t***)	130.49 (**2d2*l***)	130.95 (**2d2*d***)		133.26 (**1d**)
2/6	107.94 (**2d2*t***)	2: 114.08 (**2d2*l***)	121.3 (br)		107.41 (**1t**); 113.32 (2 of **1l**);
	107.84 (**2l2*t***)	113.97 (**2l2*l***)		0.25−0.35	113.85 (6 of **1l**, ov with 2 of **2l**);
		6: 114.5 (group of overlapping signals)			120.6 (3 d, ov)
3/5	158.75	3: 158.75	151.44 (***2d*2t**)		158.49 (1t and 3 of 1l);
		5: 151.80 (***2l*2t**)	151.30 (***2d*2l**)	1.2−1.4	151.5−151.9 (5 of 1l and 1d,
		151.67 (***2l*2l**)	151.22 (***2d*2d**)		ov with 2l and 2d)
		151.59 (***2l*2d**)			
4	108.30 (**2d2*t***)	115.03 (***2d*2l**)	122.1 (br)	0.25−0.35	106.89 (1t); 113.53 (1l);
	108.13 (**2l2*t***)	114.86 (***2l*2l**)			120.6 (1d, ov [c]))

[a] Carbon of the italicized structural unit. Relative substituent effects (in ppm): (A) due to substitution of **2d** by **2l** as preceding group, $\Delta\delta$(ipso) = + 0.26, $\Delta\delta$(ortho) = −0.1, $\Delta\delta$(meta) ≈ 0, and $\Delta\delta$(para) = −0.17; (B) due to substitution of **2d** by **2l** (or **2t**) as the following group, $\Delta\delta$(ipso) = +0.08 (+ 0.21), $\Delta\delta$(meta) ≈ 0 (0), and $\Delta\delta$(ortho) and $\Delta\delta$(para) could not be determined. [b] T_{1C} determined for a 0.5 M solution of **PDHBA** ($p_A \approx 1$) in DMSO-d_6 at 303 K. [c] ov: significant signal overlap with other signals.

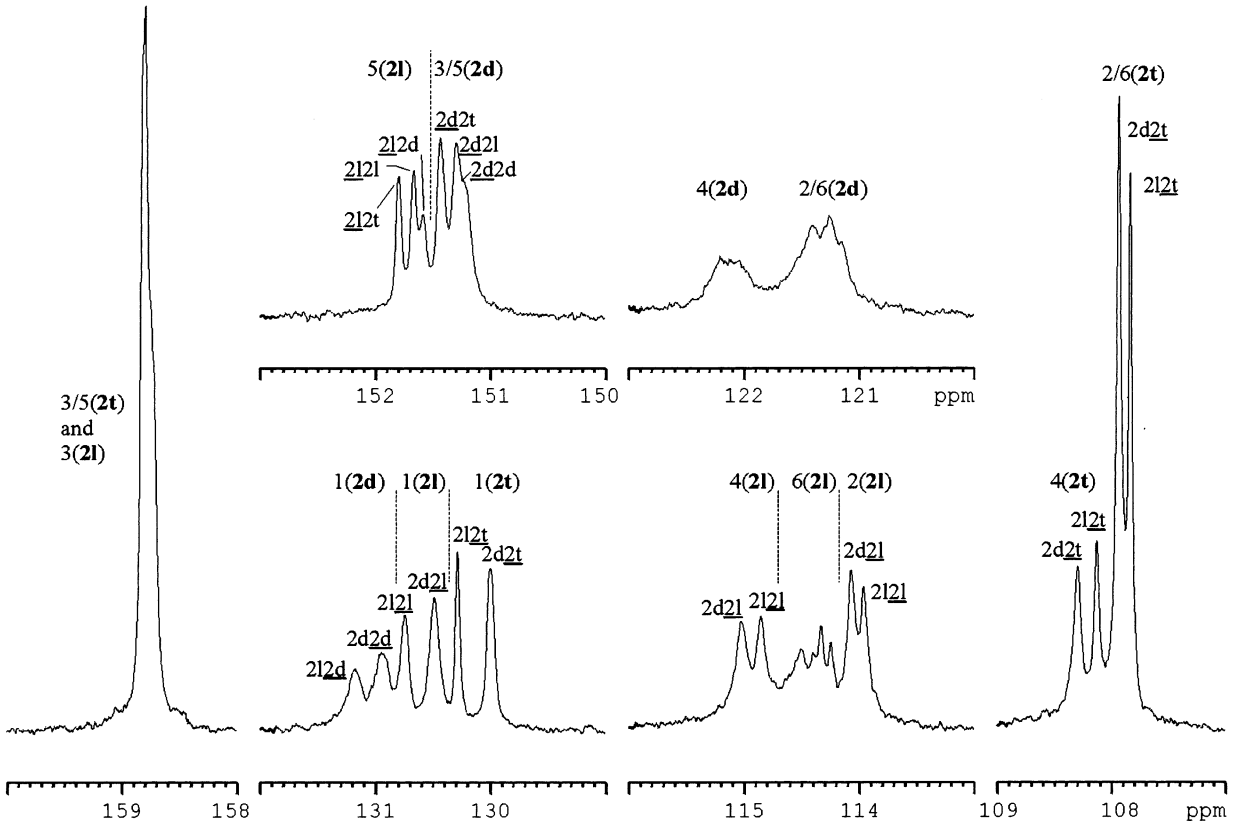

Figure 3. 125 MHz ^{13}C NMR spectrum (regions of the aromatic carbons 1−6 in Scheme 2) of **PDHBA** ($p_A \approx 1$) in DMSO-d_6 with assignments to the different structural units and partly to the diads.

polyester based on 4,4-bis(4′-hydroxyphenyl)pentanoic acid[16] and is caused by decreasing spin−spin relaxation times due to reduced segmental mobility with increasing substitution. An additional broadening may result from long-range sequence effects possible for **2l** and **2d** units.

In this paper a detailed study of ^{13}C relaxation times and nuclear Overhauser effects was not carried out, but the spin−lattice relaxation times (T_{1C}) of the different signal groups were determined (Table 2) to guarantee the quantitative analysis of the ^{13}C NMR spectra. The longest T_{1C} in our polymer solutions was determined for the carboxylic carbon of the monomer **1t** with 2.4 s.

Experimental Determination of the Conversion Dependence of the Structural Units. One can calculate the conversion of **A** functionalities p_A from the normalized ratios of the six structural units

$$p_A = 1 - \frac{\sum I(\mathbf{1})}{\sum I(\mathbf{1}) + \sum I(\mathbf{2})} = \frac{I(\mathbf{2t}) + I(\mathbf{2l}) + I(\mathbf{2d})}{I(\mathbf{1t}) + I(\mathbf{1l}) + I(\mathbf{1d}) + I(\mathbf{2t}) + I(\mathbf{2l}) + I(\mathbf{2d})} \quad (2)$$

with $I(\boldsymbol{xy})$ = normalized signal intensity of the structural units ***xy***.

Figure 4 gives a plot of the ratio of structural units as a function of the conversion p_A. For reasons of comparison, we added the data for an random polycondensation with equal reaction rate constants at each

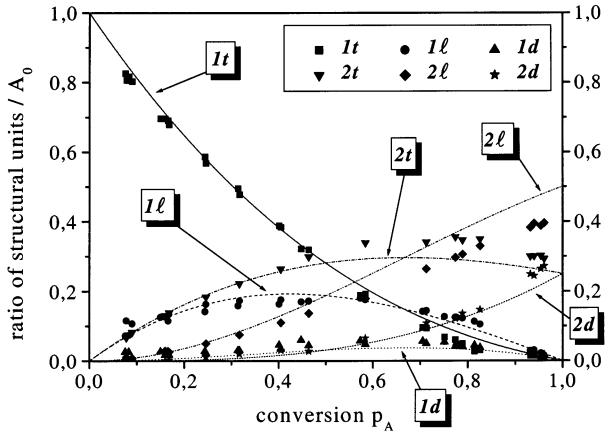

Figure 4. Conversion dependence of the structural units for the polycondensation of **BTMSBCl** (lines, theoretical data for an ideal polycondensation; symbols, NMR data; all mole fractions normalized to A_0).

step (ideal situation). The equations for the ideal polycondensation have been published elsewhere.[5,9,16]

The symbols always represent the experimental data and the lines show calculated curves. All data are represented normalized to the starting monomer concentration A_0. The absolute error is always $\leq 0.02A_0$. The relative error increases for decreasing content of a structural unit. It is obvious that our data are deviating from the ideal case and that the deviation exceeds the experimental error. A first analysis gives significant deviations for the data of **1d** at low conversion and of **1t**, **2t** and **2l** at high conversion.

The Three General Kinetic Situations. The general kinetic situation exhibits seven reaction pathways. Since there are three structural units, which contain an active **A** function and four structural units with active **B** functions one can observe 12 different basic reactions with 12 different rate constants (Table 1). We already discussed three general kinetic situations for an AB_2 system:[17]

1. The reacted **a** function decreases/increases the reactivity of the **B** functionalities (comparing columns 1 and 2 with 3 and 4, Table 1):

$$\{\mathbf{1t} \rightarrow \mathbf{1l}\} = \{\mathbf{1l} \rightarrow \mathbf{1d}\} > \{\mathbf{2t} \rightarrow \mathbf{2l}\} = \{\mathbf{2l} \rightarrow \mathbf{2d}\} \text{ (decrease)} \quad \text{(a)}$$

$$\{\mathbf{1t} \rightarrow \mathbf{1l}\} = \{\mathbf{1l} \rightarrow \mathbf{1d}\} < \{\mathbf{2t} \rightarrow \mathbf{2l}\} = \{\mathbf{2l} \rightarrow \mathbf{2d}\} \text{ (increase)} \quad \text{(b)}$$

2. The reacted **b** function decreases/increases the reactivity of the **A** function (comparing rows 1, 2 and 3, Table 1):

$$\{\mathbf{1t} \rightarrow \mathbf{2t}\} > \{\mathbf{1l} \rightarrow \mathbf{2l}\} > \{\mathbf{1d} \rightarrow \mathbf{2d}\} \text{ (decrease)} \quad \text{(a)}$$

$$\{\mathbf{1t} \rightarrow \mathbf{2t}\} < \{\mathbf{1l} \rightarrow \mathbf{2l}\} < \{\mathbf{1d} \rightarrow \mathbf{2d}\} \text{ (increase)} \quad \text{(b)}$$

3. The reacted **b** function of a linear unit decreases/increases the reactivity of the second **B** function (comparing columns 1 and 3 with 2 and 4, Table 1):

$$\{\mathbf{1t} \rightarrow \mathbf{1l}\} = \{\mathbf{2t} \rightarrow \mathbf{2l}\} > \{\mathbf{1l} \rightarrow \mathbf{1d}\} = \{\mathbf{2l} \rightarrow \mathbf{2d}\} \text{ (decrease)} \quad \text{(a)}$$

$$\{\mathbf{1t} \rightarrow \mathbf{1l}\} = \{\mathbf{2t} \rightarrow \mathbf{2l}\} < \{\mathbf{1l} \rightarrow \mathbf{1d}\} = \{\mathbf{2l} \rightarrow \mathbf{2d}\} \text{ (increase)} \quad \text{(b)}$$

The discussion of the influences in the reactivity will be based on these general kinetic situations. The general kinetic situations only contain a structural conceptualization but no chemical interpretation; they are special situations, and we expect in the real system influences of more than one reaction site. For 3,5-bis(trimethylsiloxy)benzoyl chloride (**BTMSBCl**) as monomer, all three functionalities are attached to the same benzene ring. This gives rise to the consideration that one functionality—either reacted or unreacted—can influence the reactivity of the other functional groups through inductive effects.

A chemical understanding of the reaction mechanism and the kinetics of this polycondensation is necessary prior to discussion of the experimental results.

Discussion of the Reaction Mechanism and the Reactivity of the Different Functionalities. A detailed analysis of the reaction mechanism is necessary to identify the rate-determining step. The chloride ion catalyzed polycondensation of **BTMSBCl** proceeds in three steps, two nucleophilic substitutions and the final elimination of the chloride (Scheme 3).

All three steps are possible equilibrium reactions known in silyl ether and carbonyl chemistry.[25,26] The adduct **ba*** is a highly reactive intermediate which either dissociates back or forms the ester via elimination of the chloride. The chloride elimination is not a competing equilibrium, because the nucleophilic power of the chloride is too low to attack the ester. Thus, we consider the third step as fast and irreversible. For comparison of the first two reactions we have to look at the kinetics of both the formation and the back-reaction of each step. The first reaction is the nucleophilic attack of the chloride at the silicon of the silyl ether. Since the chloride ion is a weak nucleophile, the reaction will proceed with a slow rate. At the reaction temperature (170 °C) the chlorotrimethylsilane (bp 56−57 °C) will be constantly removed to shift the equilibrium toward the side of the product, but still the equilibrium is on the side of the silyl ether.[25] The second step is the nucleophilic attack of a stronger nucleophile (the phenolate) at a highly activated and very electrophilic carbonyl group, the acid chloride. From the tetrahedral intermediate, the reaction should proceed faster toward the ester formation compared to the back-reaction, because the chloride is the better leaving group. This would lead to the assumption that the formation of the phenolate is the slowest and therefore rate-determining step. The addition of phenolate to the acid chloride is a faster step, which has only a minor kinetic effect.

From this observation, one can conclude that the formation and stability of the four different phenolates (**1t**, **1l**, **2t**, **2l**) has a major kinetic effect and the reactivity of the three different acid chlorides (**1t**, **1l**, **1d**) has only a minor kinetic effect. Thus, situations 1 and 3 or a combination of both from the three general kinetic situations would likely describe the kinetics of the system.

The electronic configuration determines which of the phenolates is the most stable one and would be most easily formed. In general, an electron-withdrawing group supports the formation of the phenolate and also stabilizes the formed phenolate. To quantify these effects the Hammett equation can be used. The Hammett equation is given in eq 3, and Table 3 gives the Hammett parameter for meta-substitution, σ_m, for the

Table 3. Hammett Constants σ_m

σ_m for a specific functional group	COCl (**A**)	COOPh (**a**)	$OSiMe_3$ (**B**)	OCOPh (**b**)
σ_m	0.51	0.37	0.13	0.21

functionalities of interest.[27]

$$\sigma = \log\frac{K_X}{K_H} \tag{3}$$

with σ = substituent constant, K_H = ionization constant for benzoic acid, and K_X = ionization constant for the corresponding meta- or para-substituted benzoic acid.

The larger σ_m is, the more electron-withdrawing is the group, and therefore, the formation and stability of the phenolate anion is preferred. With these σ_m values, one can propose a relative reactivity, as follows:

$$\{\mathbf{1t} \rightarrow \mathbf{1l}\} > \{\mathbf{2t} \rightarrow \mathbf{2l}\} \quad \text{and}$$
$$\{\mathbf{1l} \rightarrow \mathbf{1d}\} > \{\mathbf{2l} \rightarrow \mathbf{2d}\}$$
$$(\sigma_m = 0.51 \text{ vs } 0.37) \quad \text{(situation 1a)}$$

$$\{\mathbf{1l} \rightarrow \mathbf{1d}\} > \{\mathbf{1t} \rightarrow \mathbf{1l}\} \quad \text{and}$$
$$\{\mathbf{2l} \rightarrow \mathbf{2d}\} > \{\mathbf{2t} \rightarrow \mathbf{2l}\}$$
$$(\sigma_m = 0.21 \text{ vs } 0.13) \quad \text{(situation 3b)}$$

From this discussion we do not consider a major effect of the second reaction, the nucleophilic attack of the phenolate at the carbonyl group. If there is an effect, the Hammett parameter would give the following reactivity order:

$$\{\mathbf{1d} \rightarrow \mathbf{2d}\} > \{\mathbf{1l} \rightarrow \mathbf{2l}\} > \{\mathbf{1t} \rightarrow \mathbf{2t}\}$$
$$(\sigma_m = 0.21 \text{ vs } 0.13) \quad \text{(situation 2b)}$$

It is noteworthy that these calculations can only give a certain support for the discussed mechanism, because most σ values were determined for only one substituent and for molecules in solution to avoid changes in the kinetics due to limited diffusion in the system.[28] There may be a diffusion limit at high conversion since the reaction is performed in bulk (similar to regularly performed hyperbranched polycondensation reactions).

Steric effects seem unlikely for two reasons. Turner et al.[23] reported a similar system based on 3,5-bis-(acetoxy)benzoic acid, which has a DB of 50%[29] showing no reduced accessibility for highly substituted units. Also, kinetic investigations according to the Hammett parameter only consider ortho-substituted aromatic systems to change the reactivity due to steric requirements. However, steric effects of higher order due to the crowding in high molecular weight region cannot be excluded especially at high conversion.

These considerations led to a kinetic approach to fit the data, where we kept the k values constant within one column, but changed it for the different columns.

Fit of the Experimental Data and Discussion of the Ratio of Reaction Rate Constants on Basis of Chemical Reactivity. (a) Fit to the Experimental Data. The simulations were performed to fit the 12 reaction rate constants to our experimental data. Since the time component is eliminated, there are 11 independent k values giving an 11-dimensional space, where a minimum has to be found. It is quite obvious that there will be more than one local minimum. A reasonable minimum was found by performing a certain sequence of simulations. This was done using the aforementioned discussions of the kinetic situation from a chemical point of view. Running the simulations with restrictions based on the three major kinetic situations were first tests for our discussion on the influence on the chemical reactivity. Table 4 summarizes these results.

The smaller the sum of the squared errors (Table 4) the more accurate the simulation. We see a dominant influence of the kinetic situation 3. Thus, the reaction on the **B** site (trimethylsiloxy group) dominates the change in the reactivity, which is in agreement with our reaction mechanism. The result according to situation 1 is also in agreement with our discussion based on the Hammett parameter, whereas situation 2 gives a fit that gives the poorest correlation and that does not agree with the discussion on the chemical reactivity. From this result, we conclude that indeed the formation of phenolate is the rate-determining step.

In the next step, the simulation was carried out by a combination of the kinetic situations 1 and 3, which represents the overall reactivity changes on the **B** site (**K** matrix: $\boldsymbol{K}_{1+3}$). Again we can see a drop in the sum of squared errors (Table 4) indicating further improvement of our simulation. One can see that the reactivity of the unit **2t** is strongly reduced. This result seems to be an absolute minimum under the restriction of the system, because the same values can always be found independently from the starting point and method.

Finally a local minimum was identified within the previous identified region (Table 4). For the final minimization the $\boldsymbol{K}_{1+3}$ matrix of situation (1+3) was taken as a starting point. Very rigid conditions were applied for the final minimization, because in almost any situation without any boundary conditions the system diverged, giving chemically senseless results (such as $k \leq 0$). Only those data points were taken for further minimization for which the error exceeded the experimental error of $0.02A_0$. Using this restriction led to a stable value. The final result is also given in Table 4, and it is presented graphically in Figure 5.

Two different experiments were performed to prove our method. First several random **K** matrices were taken as starting matrix to minimize our experimental data and the same sequence minimizations was performed until no change is observed. Second a set of ideal data values was generated by simulating the graphs for a given **K** matrix; then, we performed the minimization sequence to check whether the same k values will be found.

(b) Discussion of the Sensitivity of Different *k* Values. It is noteworthy that certain basic reactions have a major contribution to the overall reaction and the corresponding k values give a pronounced change in shape of the simulated curves upon small changes in this particular k value. Thus, we performed a study of the sensitivity of the conversion dependence of the six structural units toward changes in a single k value. Any system of 12 k values yields a set of six functions of normalized ratio of structural units vs conversion. If a single k value is changed from $k_{\beta\alpha}$ to $k_{\beta\alpha}(1 + 10^{-n})$, one can observe a difference in all six functions. The change (or error) can be quantified by integrating the area, which the two curves enclose between $p_A = 0$ and $p_A = 1$ and summation over all six structural units

Table 4. Results of the Simulation

kinetic situation	restrictions	resulting **K** matrix	sum of squared errors	resulting final DB,[a] %
ideal situation	all k equal	$\mathbf{K}_{\text{ideal}} = \begin{bmatrix} 1 & 1 & 1 & 1 \\ 1 & 1 & 1 & 1 \\ 1 & 1 & 1 & 1 \end{bmatrix}$	0.000 80	50
situation 1	$k_{1t1t} = k_{11lt} = k_{1t1l} = k_{11ll} = k_{1t1d} = k_{11ld}$ $k_{2t1t} = k_{21lt} = k_{2t1l} = k_{21ll} = k_{2t1d} = k_{21ld}$	$\mathbf{K}_1 = \begin{bmatrix} 1 & 1 & 0.27 & 0.27 \\ 1 & 1 & 0.27 & 0.27 \\ 1 & 1 & 0.27 & 0.27 \end{bmatrix}$	0.000 52	53.2
situation 2	$k_{1t1t} = k_{11lt} = k_{2t1t} = k_{21lt}$ $k_{1t1l} = k_{11ll} = k_{2t1l} = k_{21ll}$ $k_{1t1d} = k_{11ld} = k_{2t1d} = k_{21ld}$	$\mathbf{K}_2 = \begin{bmatrix} 1 & 1 & 1 & 1 \\ 0.50 & 0.50 & 0.50 & 0.50 \\ 1.01 & 1.01 & 1.01 & 1.01 \end{bmatrix}$	0.000 55	50.0
situation 3	$k_{1t1t} = k_{2t1t} = k_{1t1l} = k_{2t1l} = k_{1t1d} = k_{2t1d}$ $k_{11lt} = k_{21lt} = k_{11ll} = k_{21ll} = k_{11ld} = k_{21ld}$	$\mathbf{K}_3 = \begin{bmatrix} 1 & 1.55 & 1 & 1.55 \\ 1 & 1.55 & 1 & 1.55 \\ 1 & 1.55 & 1 & 1.55 \end{bmatrix}$	0.000 34	58.6
situation 1+3	$k_{1t1t} = k_{1t1l} = k_{1t1d}$ $k_{11lt} = k_{11ll} = k_{11ld}$ $k_{2t1t} = k_{2t1l} = k_{2t1d}$ $k_{21lt} = k_{21ll} = k_{21ld}$	$\mathbf{K}_{1+3} = \begin{bmatrix} 1 & 1.15 & 0.62 & 1.29 \\ 1 & 1.15 & 0.62 & 1.29 \\ 1 & 1.15 & 0.62 & 1.29 \end{bmatrix}$	0.000 22	60.7
final situation	all k's varied	$\mathbf{K} = \begin{bmatrix} 1 & 1.18 & 0.68 & 1.28 \\ 1.01 & 1.17 & 0.54 & 1.21 \\ 1.01 & 1.14 & 0.64 & 1.25 \end{bmatrix}$	0.000 21	60.6

[a] Calculated after Frey's definition: $\text{DB} = 2T/(2T + L)$.

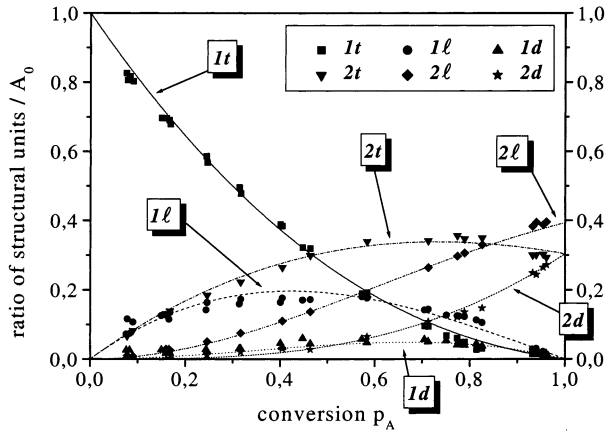

Figure 5. Conversion dependence of the structural units for the polycondensation of **BTMSBCl** (lines, fitted data using the final **K** matrix; symbols, NMR data; all mole fractions normalized to A_0).

resulting in the sensitivity parameter $\epsilon(k_{\beta\alpha},n)$.

$$\epsilon(k_{\beta\alpha},n) = \sum_{y} \int_0^1 (y - y')^2 \, \mathrm{d}p_{\mathrm{A}} \qquad (4)$$

with $\epsilon(k_{\beta\alpha},n)$ = sensitivity parameter, n = exponent of the "error" function, y = [**1t**], [**1l**], [**1d**], [**2t**], [**2l**], and [**2d**] at $k_{\beta\alpha}$, y' = [**1t**], [**1l**], [**1d**], [**2t**], [**2l**], and [**2d**] at $k_{\beta\alpha}(1 + 10^{-n})$, and p_{A} = conversion of **A** groups.

The result $y - y'$ was squared in order to count any deviation (positive or negative) in the same way. This calculation is independent from our experimental data. Obviously ϵ decreases with increasing n. $\epsilon(k_{\beta\alpha},n)$ changes also depending on the applied **K** matrix, but the order remains the same within a wide range of k values. There are large differences of $\epsilon(k_{\beta\alpha},n)$ between different $k_{\beta\alpha}$ values. These differences are within 2 orders of magnitude. The parameter is called sensitivity because it is an indicator of how small changes in $k_{\beta\alpha}$ affect the concentration of the reactants throughout the reaction. For the problem of fitting a curve to experimental data by changing the k values, one can see that the k values with high sensitivity have a strong influence on all six concentration curves allowing an easier fitting process. Speaking in terms of identifying a minimum in the 11-dimensional space of k values: High $\epsilon(k_{\beta\alpha},x)$ leads to steep curvature in the corresponding $k_{\beta\alpha}$ direction and low $\epsilon(k_{\beta\alpha},x)$ leads to an almost flat region. In conclusion, the larger $\epsilon(k_{\beta\alpha},x)$ is for a given x, the more sensitive is the k value $k_{\beta\alpha}$ and the better a minimum can be found. Taking large n's ($n > 6$), we found a linear relationship between $\log\{\epsilon(k_{\beta\alpha},n)\}$ and n, where every $\epsilon(k_{\beta\alpha})$ has always the same slope, equaling 2.[30]

The previous observation directly influences the accuracy of our determined **K** matrix and gives certain consideration for the interpretation of our results.

A given **K** matrix has always a corresponding matrix of 12 $\epsilon(k_{\beta\alpha}, n)$ values (**E** matrix). (n has to be kept constant for calculating the **E** matrix. Since the values for the ϵ value are dependent from the chosen n, we normalized the **E** matrix for the largest ϵ value. All given **E** matrices are calculated with $n = 8$.) These 12 values scale the inherent error of our results. Translated into the underlying chemical reaction, one can say that certain basic reaction step can be identified as very important, because it contributes largely to the overall reaction, others are less important. Fortunately, the important reactions for fitting the data (mathematical aspect) are also those, which have the largest contribution to the overall reaction (chemical aspect). When both reaction partners are in very low concentrations throughout the entire reaction, these basic reactions are less important and we find the k value with a larger error due to the low sensitivity. (The relation between the concentrations and the sensitivity is only a rough estimation, which gives the order of magnitude but not the real sensitivity data.) A graph of incremental change vs conversion for the 12 basic reactions is shown in the appendix taking the final **K** matrix in order to visualize

this correlation.

Concluding this section, one can say that the higher the sensitivity is the lower is the error in determining the particular k value and the more important is this reaction. When the data are minimized according to the above-mentioned discussion on the reactivity changes by keeping all k values equal within one column, the system becomes very robust, because all sensitivities are in the same range.

The results of the sensitivity study are given for the $\boldsymbol{K}_{1+3}$ and for the final **K** matrix (eqs 5 and 6).

$$\mathbf{K}_{1+3} = \begin{bmatrix} 1 & 1.15 & 0.62 & 1.29 \\ 1 & 1.15 & 0.62 & 1.29 \\ 1 & 1.15 & 0.62 & 1.29 \end{bmatrix}, \quad \text{with}$$

$$\mathbf{E}_{1+3} = \begin{bmatrix} 1 & 0.588 & 1.37 & 1.08 \\ 1 & 0.588 & 1.37 & 1.08 \\ 1 & 0.588 & 1.37 & 1.08 \end{bmatrix} \quad (5)$$

$$\mathbf{K} = \begin{bmatrix} 1 & 1.18 & 0.68 & 1.26 \\ 1.01 & 1.17 & 0.54 & 1.21 \\ 1.01 & 1.14 & 0.64 & 1.25 \end{bmatrix}, \quad \text{with}$$

$$\mathbf{E} = \begin{bmatrix} 1 & 0.242 & 0.197 & 0.248 \\ 0.172 & 0.074 & 0.353 & 0.015 \\ 0.015 & 0.005 & 0.034 & 0.046 \end{bmatrix} \quad (6)$$

Going over from $\boldsymbol{K}_{1+3}$ to the final **K** matrix was done using very rigid minimization conditions. Comparison of eqs 5 and 6 shows the reason. Some of the k values are very insensitive, which means they can be changed within a wide range without a noticeable effect on the shape of the curves. These conditions have been applied in order to avoid a diverging situation. Thus, eq 6 represents a local minimum found using $\boldsymbol{K}_{1+3}$ as starting condition.

Analysis and Simulation of the Diads. (a) Pathways for the Formation of the Diads. As shown in the NMR part, we observed an additional fine structure for the peaks of the structural units, e.g. the three carbonyl peaks of **2t**, **2l**, and **2d** appear as two separate peaks each. This fine structure could be attributed to the effect on the chemical shift of different penultimate groups depending whether the penultimate group is a linear or a dendritic group. Therefore, a further analysis of our data has been carried out. One can distinguish 12 diads by combining the four penultimate groups ***x*(l,d)** (x = **1**, **2**) with the three **2*y*** units. In our special case we could not distinguish between **1(l,d)** and **2(l,d)** as penultimate group by NMR spectroscopy. This reduces the total number of observed diads to six, where always the sum of two diads are given (e.g., **L2t** = **1l2t** + **2l2t**). Scheme 4 shows the notation and the reaction pathways of these six diads.

These six diads were measured and quantified as a function of the conversion by quantitative ^{13}C NMR spectroscopy. The next section compares the experimental data with the results from previous simulation in order to evaluating the microstructure and higher order kinetic effects.

(b) Simulation and Fit of the Diad Content to the Experimental Data. The discussion of the diads is directed toward the question whether we have further effects on the kinetics, which go beyond the differences in the reactivity of the 12 bimolecular reactions; e.g., steric effects cannot be excluded for this very dense structure. The conversion dependence of the six diads was calculated based on the previous evaluated k values.

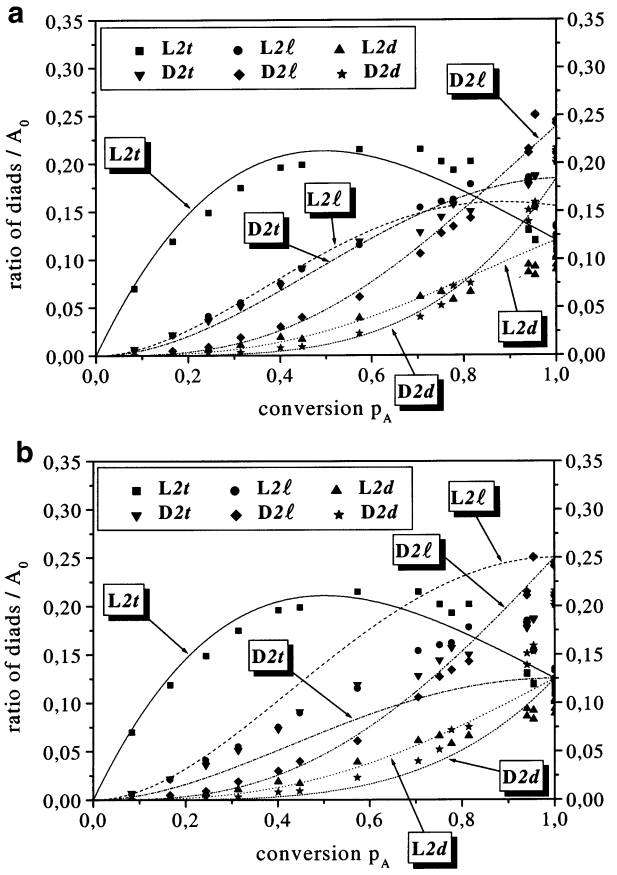

Figure 6. Conversion dependence of the diads for the polycondensation of **BTMSBCl** compared to calculated curves using (a) the final **K** matrix and (b) theoretical data for an ideal polycondensation (lines, calculated curves; symbols, NMR data; all mole fractions normalized to A_0).

The simplest approach, without making any further kinetic considerations, is the calculation of the diad content as a product of the two structural units normalized to the total number of diads.[17]

The equations for the calculation of the content of our six measured diads based on the six structural units are given in the Supporting Information. This approach considers different reaction ratios for the formation of the structural units, but it calculates the diad distribution as a probability distribution based on the previous calculated **K** matrix. This probability distribution has already been successfully applied to the system of 4,4-bis(4′-hydroxyphenyl)pentanoic acid, which shows an ideal conversion dependence of the diads.[16] In Figure 6a, we compare our experimental data with plots of fitted curves based on the final **K** matrix.

Since the monomeric units already show a deviation from the ideal statistical distribution, it is expected that also the diad ratio deviate from the ideal case. A comparison of the experimental data with the curves of the ideal case is shown in Figure 6b. It indicates clearly that these deviations of diad content exceed the experimental error. The calculation of the curves for the diads using our data set of reaction rate constants shows a good fit. The content of the **L2l** diads is substantially decreased whereas the amount of **D2t** and **D2d** is increased above the values for the ideal statistical situation. The relatively high content of **D2d** diads reflects a substantially denser microstructure of this hyperbranched polymer compared to a hyperbranched polymer, which has an ideal distribution of structural

units and diads. This might effect the molecule shape and the physical and chemical properties to a certain extent.[31]

For the discussion of the diads it has to be considered that the relative error for our experimental data is a little higher compared to that for the data of the structural units. On the one side the absolute values are smaller and on the other side the data were obtained by signal deconvolution of two overlapping signals, which also decreases the accuracy. Minor kinetics effects on the diad formation may not be found.

Analysis of the Degree of Branching. The degree of branching (DB) is another tool to describe the microstructure and the polymer architecture compared to purely linear polymers (DB = 0) and perfectly branched dendrimers (DB = 100%), respectively. Since most of our data refer to oligomers, we will only discuss the DB calculated applying the definition of Frey et al.[8] (eq 7).

$$\mathrm{DB} = \frac{2D}{2D + L} \tag{7}$$

Again, the calculation of DB is based on the fit of the reaction rate constants for our experimental data of the structural units, which yields in a good agreement between fit and experimental DB. Deviations at low conversion ($p_A = 0-0.4$, $\bar{P}_n = 1 - 1.7$) reflect a larger experimental error, because the dendritic units are at a very low concentration. Figure 7 gives a plot of DB vs the conversion p_A and vs the degree of polymerization $\bar{P}_n$.

The DB exceeds the value 50%, expected for an ideal statistical situation, at conversion $p_A \approx 0.93$, which correspond to a degree of polymerization $\bar{P}_n \approx 15$ ($\bar{M}_n \approx$ 2800 g/mol).[32] The analysis of the degree of branching and of the diads are first steps toward a deeper understanding of the internal structure of the hyperbranched polyester, obviously certain questions cannot be answered due to averaging over all structural units and diads. So, the distribution of the structural units and diads over different polymer molecules and their radial distribution within one polymer molecule are of interest.

Conclusions

On the basis of our previous theoretical discussion on the kinetics of nonideal hyperbranched polymerizations, we were able to present an application of this theoretical work when evaluating the kinetic data of the polycondensation of 3,5-bis(trimethylsiloxy)benzoyl chloride (**BTMSBCl**). NMR spectroscopy provided an excellent tool for the qualitative and quantitative evaluation of the data. A complete signal assignment of the structural units has been achieved on the resulting **PDHBA**, where all TMS and acid chlorid groups have been hydrolyzed. Furthermore, the signal fine structure could be attributed to the influence of the following and the penultimate group leading to the determination of the diads. Computer simulation in conjunction with a chemical interpretation of these results led to a good fit of the experimental data to the simulated curves. The Hammett parameters provide a tool to support our chemical interpretation. We found that the formation and stability of the phenolate is the rate determining effect. The addition of the acid chloride to the phenolate only has a marginal effect on the kinetics. Through a

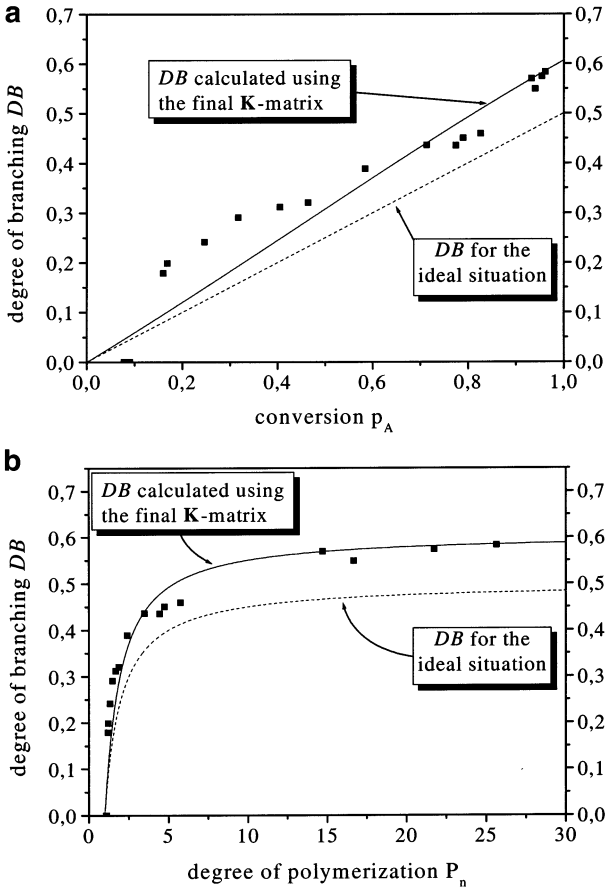

Figure 7. Degree of branching DB_{Frey} for the polycondensation of **BTMSBCl** compared to calculated curves using the final **K** matrix and the data for an ideal statistical polycondensation (lines, simulated data; symbols, DB calculated from NMR data): (a) DB vs conversion p_A; (b) DB vs degree of polymerization $\bar{P}_n$.

sequence of simulations using the least-mean-squares method, the minimized **K** matrix was determined to be

$$\mathbf{K} = \begin{bmatrix} 1 & 1.18 & 0.68 & 1.26 \\ 1.01 & 1.17 & 0.54 & 1.21 \\ 1.01 & 1.14 & 0.64 & 1.25 \end{bmatrix}$$

which basically reflects a major accelerating effect of the reacted **b** function on the reactivity of the second **B** function (situation 3b, $\{\mathbf{T} \rightarrow \mathbf{L}\} < \{\mathbf{L} \rightarrow \mathbf{D}\}$) and a minor rate increasing effect of the unreacted **A** function on the reactivity of the **B** function (situation 1a, $\{\mathbf{1(t,l)} \rightarrow \mathbf{1(l,d)}\} > \{\mathbf{2(t,l)} \rightarrow \mathbf{2(l,d)}\}$). Both rate accelerations are due to preferred formation of the most stable phenolate.

Further information about the microstructure were obtained from the diad determination in addition to the calculation of the degree of branching, but could not detect any further kinetic effect, which go beyond the formation of the single structural units. Thus, steric effects on the kinetics can be excluded so far.

Acknowledgment. The authors thank Dr. P. Friedel, Prof. A. H. E. Müller, and Dr. H. Frey for helpful discussion.

Supporting Information Available: Text and figures referring to the sensitivity studies, studies on the relative weight of the different reactions, studies on the diads, equations for the calculation of the diad content, and comparison

of the data with the ideal kinetic situation. This material is available free of charge via the Internet at http://pubs.acs.org.

References and Notes

(1) Flory, P. *J. Am. Chem. Soc.* **1952**, *74*, 2718.
(2) Hawker, C. J.; Lee, R.; Fréchet, J. M. J. *J. Am. Chem. Soc.* **1991**, *113*, 4583−4588.
(3) Kim, Y. H.; Webster, O. W. *Macromolecules* **1992**, *25*, 5561−5572.
(4) Müller, A. H. E.; Yan, D.; Wulkow, M. *Macromolecules* **1997**, *30*, 7015−7023.
(5) Yan, D.; Müller, A. H. E.; Matyjaszewski, K. *Macromolecules* **1997**, *30*, 7024−7033.
(6) Radke, W.; Litvinenko, G.; Müller, A. H. E. *Macromolecules* **1998**, *31*, 239−248.
(7) Litvinenko, G.; Simon, P. F. W.; Müller, A. H. E. *Macromolecules* **2001**, *34*, 2418−2426.
(8) Hölter, D.; Burgath, A.; Frey, H. *Acta Polym.* **1997**, *48*, 30−35.
(9) Hölter, D.; Frey, H. *Acta Polym.* **1997**, *48*, 298−309.
(10) Hanselmann, R.; Hölter, D.; Frey, H. *Macromolecules* **1998**, *31*, 3790−3801.
(11) Beginn, U.; Drohman, C.; Möller, M. *Macromolecules* **1997**, *30*, 4112−4116.
(12) Dušek, K.; Šomvársky, J.; Smrcková, M.; Simonsick, W. J.; Wilczek, L. *Polym. Bull. (Berlin)* **1999**, *42*, 489−496.
(13) Cameron, C.; Fawcett, A. H.; Hetherington, C. R.; Mee, R. A. W.; McBride, F. V. *Chem. Commun.* **1997**, 1801−1802.
(14) Cameron, C.; Fawcett, A. H.; Hetherington, C. R.; Mee, R. A. W.; McBride, F. V. *J. Chem. Phys.* **1998**, *108*, 8235−8251.
(15) Galina, H.; Lechowicz, J. B.; Kaczmarski, K. *Macromol. Theory Simul.* **2001**, *10*, 174−178.
(16) Schmaljohann, D.; Komber, H.; Voit, B. I. *Acta Polym.* **1999**, *50*, 196−204.
(17) Schmaljohann, D.; Barratt, J. G.; Komber, H.; Voit, B. I. *Macromolecules* **2000**, *33*, 6284.
(18) Schmaljohann, D.; Häussler, L.; Pötschke, P.; Voit, B. I.; Loontjens, J. A. *Macromol. Chem. Phys.* **2000**, *201*, 49−57.
(19) Thompson, D. S.; Markoski, L. J.; Moore, J. S. *Macromolecules* **1999**, *32*, 4764−4768.
(20) Magnusson, H.; Malmström, E.; Hult, A. *Macromolecules* **2000**, *33*, 3099−3104.
(21) Kricheldorf, H. R.; Zang, Q.-Z.; Schwarz, G. *Polymer* **1982**, *23*, 1821.
(22) Wooley, K. L.; Hawker, C. J.; Lee, R.; Fréchet, J. M. J. *Polym. J.* **1994**, *26*, 187−197.
(23) Turner, S. R.; Voit, B. I.; Mourey, T. H. *Macromolecules* **1993**, *26*, 4617−4623.
(24) Komber, H.; Böhme, F.; Pospiech, D.; Rätzsch, M. *Makromol. Chem.* **1990**, *191*, 2675−2684.
(25) Kricheldorf, H.; Schwarz, G. *Makromol. Chem.* **1983**, *184*, 475−496.
(26) Sykes, P. *Reaktionsmechanismen der Organischen Chemie*, 9th ed.; VCH: Weinheim, Germany, 1988; pp 276−281.
(27) Hansch, C.; Leo, A.; Taft, R. W. *Chem. Rev.* **1991**, *91*, 165−195.
(28) Logan, S. R. *Fundamentals of Chemical Kinetics*, 1st ed.; Longman: London, 1996; pp 94−96.
(29) This determination of DB was performed on a hydrolyzed sample; recently we were able to confirm this result by quantitative ^{13}C NMR (Komber, H., 1999, unpublished result).
(30) Barratt, J. G. 2000, unpublished results.
(31) Wooley, K. L.; Fréchet, J. M. J.; Hawker, C. J. *Polymer* **1994**, *35*, 4489−4495.
(32) This is the first data point with a DB higher than 50%, the simulation led to exceeding 50% at $p_A = 0.81$, $\bar{P}_n = 5.3$.

MA020972M